A COMPUTATIONAL COMPARISON BETWEEN LINEAR AND PULSED EXTRACORPOREAL MEMBRANE OXYGENATION (ECMO) BASED ON HEMODYNAMICS IN THE AORTA

Vera Gramigna[(a)], Maria Vittoria Caruso[(b)], Attilio Renzulli [(c)], Gionata Fragomeni [(d)]

[(a) (b) (d)] Department of Computer and Biomedical Engineering, *"Magna Graecia"* University, Catanzaro, 88100, Italy
[(c)] Cardiac Surgery Unit, *"Magna Graecia"* University, Catanzaro, 88100, Italy

[(a)]gramigna@unicz.it, [(b)]mv.caruso@unicz.it, [(c)]renzulli@unicz.it, [(d)]fragomeni@unicz.it

ABSTRACT

The experience of combining extra-corporeal membrane oxygenation (ECMO) with intra-aortic balloon pump (IABP) for the treatment of acute heart failure in critically ill adults can in principle have a synergistic and complementary effect. ECMO is a medical procedure used to supply oxygen to the blood circulation of patient with cardiac/ pulmonary failure. Since linear flow in ECMO is often responsible for some clinical problems, aim of this study was to evaluate the hemodynamic difference in the aorta due to linear and pulsed ECMO, the latter obtained with the IABP, currently the most commonly used mechanical circulatory support device. A multiscale model, realized coupling a 3D CFD analysis with a lumped parameters model (resistance's boundary conditions), was carried out. The numerical results showed that the aortic flow followed the balloon radius behavior's change. Therefore pulsatility similar to the arterial one, in respect of the linear standard behaviour (IABP not inserted), occurred.

Keywords: Extracorporeal Membrane Oxygenation (ECMO), Intra Aortic Balloon Pump (IABP), Computation Fluid Dynamic (CFD), Multiscale Model

1. INTRODUCTION

In the last years, the limitations of the most commonly methods (such as the extra-corporeal membrane oxygenation -ECMO- and the intra-aortic balloon pump -IABP-) which were unable, if used singularly, to achieve ideal outcomes in patients with severe disease, contributed to diffusion of technique that combine the two methodologies for the treatment of acute heart failure in adults. In fact, even if the IABP can improve blood flow to internal organs, allowing the weakened heart to recover its function, it cannot replace the physiological pumping of the heart. For patients whose cardiac muscle is already severely damaged, IABP support may not raise cardiac output sufficiently to meet the body's needs, creating the necessity for further circulatory support (Pengyu 2014). The principle of ECMO, long-term extracorporeal support used to treat patients with severe cardiac/ pulmonary failure, is based on prolonged partial cardiopulmonary bypass. When the ECMO is used to keep the heart at rest, the connection aorta - right atrium is adopted and the two cannulas are inserted via surgical cut down. Even if the survival rate is high, cerebrovascular injury may be an important complication. In fact, the significant changes in cerebral circulation that happen during induction of ECMO (decreased arterial pulsatility and rapid changes in arterial partial pressure of oxygen and carbon dioxide) compared with the previous state (patient is hypoxemic for hours), are often responsible for cerebral damage (Papademetriou 2011) .

Mathematical methods and Computational Fluid Dynamics (CFD) have recently emerged as a powerful design tool in hemodynamic context. Different studies were focused on the CFD-based design strategies applied to blood flow in pumps and other blood-handling devices (Behbahani 2009). Nevertheless little is known about fluid dynamics changes in aorta during IABP- induced pulsed ECMO.

The aim of this study was to investigate the flow pattern in the ascending aorta and in the epiaortic vessels between non-pulsatile standard ECMO (linear and constant flow) and pulsatile ECMO (induced by IABP) in a computational fluid dynamics (CFD) model and to look for hemodynamic differences. In the present study, flow pulsatility during CPB was realized through the use of the IABP, whose principal component is a polyethylene balloon which inflates and deflates according to the cardiac cycle (Biglino 2010).

2. MATERIALS AND METHODS

2.1. ECMO Circuit

The principal components of the ECMO circuit considered in this study were: a Stöckert Centrifugal Pump (SCP) combined with the Stöckert Centrifugal Pump Console (Stockert Instrumente GmbH, Munich,

Germany), a membrane oxygenator (Quadrox D, Maquet, Jostra) with integrated heart exchanger, an oxygen/air blender, and an oximetry monitor.

2.2. The geometrical model

A 3D real patient-specific model of the aorta was obtained from a series of in vivo contrast-enhanced axial CT-scan slices, done for clinical reasons. The medical images used in the present study were a collection of DICOM files and the reconstruction of three-dimensional model was performed through a process of semiautomatic segmentation using a commercial open source software (Itk snap software, http://www.itksnap.org). Finally, the derived faced surface was simplified for the CFD analysis using the reverse engineering process (Figure 1). Informed consent was granted for the patient, before enrolling him in the research.

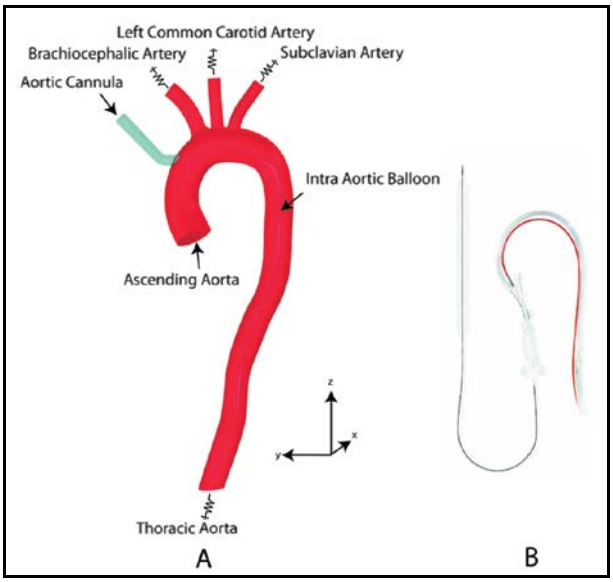

Figure 1: Multiscale model (A) and used IABP (B). The model includes the arterial cannula, the deflated IABP and the lumped parameters model (resistance's boundary conditions) used for the four vessels.

The model reproduced the ascending aorta, the three epiaortic vessels (innominate or brachiocephalic artery, left common carotid artery, left subclavian artery), and the thoracic aorta.

A standard ECMO arterial cannula (24 Fr Medtronic Inc., Minneapolis, MN, USA) was added to the ascending aorta on the site that is routinely adopted at our institution (Cardiothoracic Surgery Unit, Department of Medical and Surgical Sciences), 2 cm below the take off of the innominate artery on the anterior wall of the aorta and with a tilt angle of 45° (Figure 1).

To reproduce the physiological flow pulsatility, the Intra Aortic Balloon Pump (IABP) was used (Chang 2010, Lim 2013). Its principal component is a polyethylene balloon placed after the left subclavian artery and before the iliac bifurcation, which inflates and deflates according to the cardiac cycle: it is fully inflated in mid diastole and fully deflates in systolic peak. The intra-aortic balloon (Sensation 7 Fr. 40 cm3 with CS300 IABP System, Datascope, Maquet GmbH and Co. KG, Rastatt, Germany) was set in the descending aorta (Biglino 2010), 2 cm below the left subclavian artery, as in clinical practice (Onorati et al. 2009a, 2009b and 2009c) (Figure 1). The geometry was simplified ignoring the conical terminal parts and considering only the central cylinder, with a volume of 0.9 ml in deflation phase and of 38.7 ml at the full inflated instant, giving an 84% lumen obstruction in the descending aorta (Biglino 2010, Kem 1999, Lim 2013).

2.3 Mathematical model, boundary conditions and simulations details

Blood was considered as a Newtonian flow (Quarteroni 2000, Vignon-Clementel 2006, Formaggia 2009, Gao 2005) whose motion was described using the three-dimensional incompressible Navier-Stokes equations:

$$\nabla \cdot \mathbf{u} = 0 \quad (1)$$

$$\rho\,(\partial \mathbf{u}/\partial t) + \rho(\mathbf{u}\cdot\nabla)\mathbf{u} = \nabla\cdot[-p\mathbf{I} + \mu(\nabla\mathbf{u} + (\nabla\mathbf{u})^{T}] + \mathbf{F} \quad (2)$$

where **u** represented the fluid velocity vector, p the pressure, μ the dynamic viscosity, ρ the density of blood, **I** the identity matrix and **F** the volume force field, which was neglected in the computational study because the effect of gravity was ignored (the patient was supine during the surgical procedure). ρ and μ were equal to 1060 Kg/m^3 and 0.0035 Pa·s, respectively.

Moreover, in this study was hypothesized that the all flow delivered only through the ECMO arterial cannula (continuous flow of 5.5 L/min) and the aorta was considered as clamped (no flow came out from aortic valve). The laminar model was chosen to simulate the blood flow motion because, with a flow of about 5.5 L/min, the Reynolds number was about 3400 in arterial cannula and about 1200 in ascending aorta.

Considering an assistance level of 1:1, the balloon inflation behaviour was approximated with an 8 degree Fourier general model. The balloon inflation started 0.2 s after the beginning of the diastole and the maximum volume was reached in 0.25 s, considering a cardiac cycle of about 1 s, so a “false” systolic peak, due to IABP, occurred at 1.45 sec. Moreover, the balloon displacement in the x, y directions was controlled by a parametric solver.

A multiscale study, realized coupling a 3D CFD analysis and a lumped parameters model (0D boundary conditions), was carried out by using COMSOL 4.3a (COMSOL Inc, Stockholm, Sweden), a finite-element-based commercial software package.

As inlet boundary condition, a continuous flow value of 5.5 L/min, delivered through the arterial cannula, was used, while as outlet boundary conditions (Vignon-Clementel 2006a, 2006b), a 0D model made only of resistances (Lee 2002, Olufsen 2000, Benim 2011) was adopted to represent the arterial system of

the downstream branch regions (smaller arteries, arterioles, capillaries, venules and veins). Resistances at the four outflow exits (innominate artery, left common carotid artery, left subclavian artery and thoracic aorta) were imposed by the following pressure equation:

$$p=p_0+R\cdot Q \quad (3)$$

where p_0 was an aortic outlet pressure of 80 mmHg, Q indicated the instantaneous volumetric flow rate through each respective outflow exits, calculated at each time instant from the local velocity profile, and R the resistance. We used a constant outlet pressure offset of 80 mmHg to obtain a physiologically range of pressures in the system. R values were optimized for each vessel in order to create a referential model, characterized by the real flow rates, for every patient in the same circumstances: $2.9\cdot10^8$ Pa·s/m^3 for the brachiocephalic artery, $6.0\cdot10^8$ Pa·s/m^3 for left common carotid and left subclavian arteries and $0.6\cdot10^8$ Pa·s/m^3 for the thoracic aorta.

Moreover the vessel and the arterial cannula walls were assumed to be rigid and no-slip boundary conditions were applied.

Mesh was assessed in order to obtain a good quality for linear and pulsed cases and included two boundary layers and tetrahedral elements: 75980 elements for first case and 367742 elements for second case. The different number of elements occurred because in linear case (without IABP) tridimensional models consisted only of the aorta anatomy and the arterial cannula, while in assisted one there was also the balloon in the descending aorta.

For the fluid-dynamic analysis, to evaluate the blood flow perfusion in the aorta and epiaortic vessels, two time-depending parametric simulations were performed and the Pardiso solver was used to solve the Navier-Stokes equations. The P1-P1 finite element method was used for the space discretization in the equations of the blood motion. For all simulations three balloon inflation phase were considered to eliminate the transitory initial effects and only one was analyzed (from 2 to 3 sec).

Hemodynamic parameters for all vessels were evaluated and the comparison between linear and IABP-induced pulsatile ECMO flow rates was assumed as index of epiaortic perfusion improvement.

3. RESULTS AND DISCUSSIONS

Flow rates in inflation instant for each vessel in linear and pulsed ECMO were evaluated and percent flow (%) in respect to the aortic cannula flow of 5.5 L/min were calculated (Table1). Moreover hemodynamic changes between linear and pulsed ECMO were analyzed during the cardiac cycle by means of percent error (P-L) between linear (L) and pulsed (P) ECMO. In the inflation instant, considered as a “false” systolic peak, IABP produced an increase of flow rates in all epiaortic vessels, with a mean value of about 12.87%, 13.81%, 16.18% in brachiocephalic, left common carotid and left subclavian arteries, respectively. Moreover, the presence of IABP produced pulsatility in the flow behavior, as in physiological case, but with lowest peak value of each vessel (Figure 2).

Table 1: Flow Rate in the inflation instant for each vessel in linear and pulsed ECMO and percentage difference (P-L) between the two cases. I: Ascending Aorta; II: Brachiocephalic Artery; III: Left Common Carotid Artery; IV: Left Subclavian Artery; V: Thoracic Aorta.

Vessel	LINEAR (L)		PULSED (P)		P - L
	[L/min]	%	[L/min]	%	%
I	0,00	0,00	0,01	0,12	0,12
II	1,04	18,86	1,75	31,73	12,87
III	0,74	13,43	1,50	27,24	13,81
IV	0,87	15,84	1,76	32,01	16,18
V	2,48	45,03	0,46	8,34	-36,69

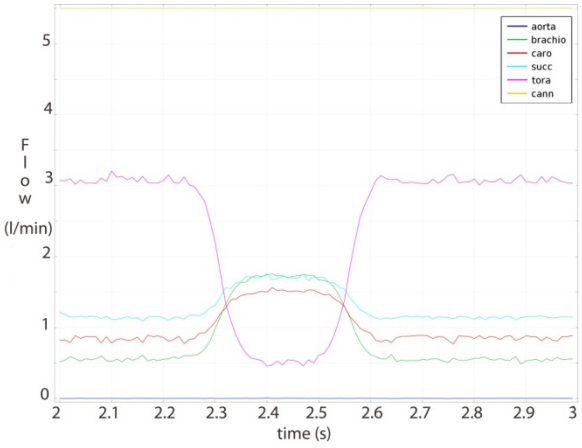

Figure 2: Flow distribution (l/min) during one IABP cycle

Analyzing streamlines behavior in aortic model, Figure 3 highlighted a dramatic difference in the blood flow dynamic through the epiaortic vessels between linear (A) and pulsed case (B and C). In fact in the first case the flow hit the inner wall of aortic arch and headed to thoracic aorta, while in the second case the flow was directed to the subclavian artery and thoracic aorta when the balloon was deflated, and to the left common carotid and left subclavian arteries in deflation phase. Moreover, the counterpulsation in inflation phase produced a steady flow pattern in each epiaortic vessel, which, on the contrary, appeared whirling in the linear case.

This model allowed the study of hemodynamic parameters in a model of aorta in linear situation and in presence of IABP during ECMO. Moreover, it could be allow quantitative prediction of hemolysis and supports the engineer in identifying recirculation areas and other regions with an increased probability for blood clotting (Behbahani 2009).

4. LIMITATIONS AND FUTURE PERSPECTIVES

Although the main contribution of this work was the implementation of a 3D-0D model to evaluate the modifications of aortic hemodynamics during IABP pulsed ECMO, it presents several limitations.

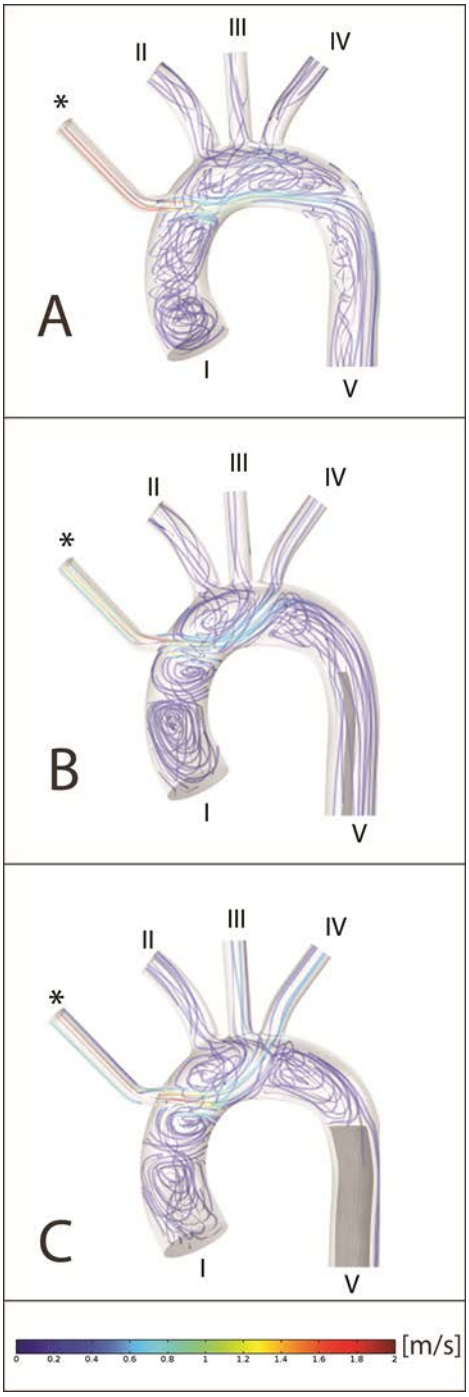

Figure 3: Velocity stream lines (m/s) during the aortic cross-clamp time in control case (A) ECMO-IABP off- and in the pulsed case: (B) ECMO-IABP on- at the deflation instant and (C) ECMO-IABP on- at the inflation instant. I: Ascending Aorta; II: Brachiocephalic Artery; III: Left Common Carotid Artery; IV: Left Subclavian Artery; V: Thoracic Aorta; *: Aortic cannula.

First the resistance values were supposed constant during assisted cases, but it was not true in real situations (Onorati et al. 2009a, 2009b and 2009c). For example, as reported in (Krishna et al. 2009), balloon inflation during diastole causes displacement of the stroke volume, and hence activation of the aortic baroreceptors. The peripheral resistance is reduced, thus improving blood flow. This resistance change was not taken into account in our study. Thus, the improvement of the present model would be the estimation of resistance values and their behavior during cardiac cycle, by means, for example, of a pressure-drop model (Itu L. et al. 2012). Moreover it would also be useful to study a multiscale fluid-structure simulation to analyze vascular wall modification in pathological cases. The idea will be to use results obtained from *ex-vivo* experimental tensile tests on aortic tissue as data of structural mechanical behavior and of wall deformation laws.

REFERENCES

Behbahani, M., 2009. A Review of Computational Fluid Dynamics Analysis of Blood Pumps. *European Journal of Applied Mathematics*, 20, 363–397.

Benim, A.C., Nahavandi, A., Assmann, A., Schubert, D., Feindt, P., Suh, S.H., 2011. Simulation of blood flow in human aorta with emphasis on outlet boundary conditions. *Applied Mathematical Modelling*, 35(7), 3175-3188.

Biglino G., 2010. *Experimental study of the mechanics of the intra-aortic balloon*. Thesis (Ph.D). Brunel University.

Chang Y., Bin G., 2010. Modeling and identification of an intra-aorta pump. *ASAIO J*, 56(6):504-9.

Datascope Corp. *Sensation 7Fr. IAB Catheter, Instructions for use*, Maquet. Available from: http://ca.maquet.com/clinicianinformation/instructions-for-use/iab-catheters/ [accessed 10 April 2013].

Formaggia, L., Quarteroni, A., Veneziani, A., 2009. *Cardiovascular Mathematics, Modeling and simulation of the circulatory system*, Volume 1, Springer. Milan.

Gao, F., Watanabe, M., Matsuzawa, T., 2005. Three-dimensional Computational Mechanical Analysis for 3-layered Aortic Arch Model under Steady and Unsteady Flow with Fluid-structure Interactions. *Proceedings of the Eighth International Conference on High-Performance Computing in Asia-Pacific Region, IEEE Computer Society*. pp. 161. November 30-December 03, Beijing, (China).

Itu L., Sharma P., Ralovich K., Mihalef V., Ionasec R., Everett A., Ringel R., Kamen A., Comaniciu D., 2012. Non-Invasive Hemodynamic Assessment of Aortic Coarctation: Validation with In Vivo Measurements. *Annals of Biomedical Engineering*, 41(4), 669–681.

Kern M. J., Aguirre F. V., Caracciolo E. A., Bach R. G., Donohue T. J., Lasorda D., Ohman E. M., Schnitzler R. N., King D. L., Ohley W. J., Grayzel

J., 1999. Hemodynamic effects of new intra-aortic balloon counterpulsation timing methods in patients: a multicenter evaluation. *American Heart Journal*, 137, 1129-1136.

Krishna M., Zacharowsk K., 2009. Principles of intra-aortic balloon pump counterpulsation. *Continuing Education in Anaesthesia, Critical Care & Pain*, 9(1), 24-28.

Lee, D., Chen, J.Y., 2002. Numerical simulation of steady flow fields in a model of abdominal aorta with its peripheral branches. *Journal of Biomechanics*, 35 (8), 1115–1122.

Lim K. M.., Lee J. S., Gyeong M.-S., Choi J.-S., Choi S. W., Shim E. B., 2013. Computational Quantification of the Cardiac Energy Consumption during Intra-Aortic Balloon Pumping Using a Cardiac Electromechanics Model. *Cardiovascular Disorders*, 28, 93-99.

Olufsen, M.S., Peskin, C.S., Kim, W.Y., Pedersen, E.M., Nadim, A., Larsen J., 2000. Numerical simulation and experimental validation of blood flow in arteries with structured-tree outflow conditions. *Annals of Biomedical Engineering*, 28(11), 1281-1299.

Onorati, F., Santarpino, G., Presta, P., Caroleo, S., Abdalla, K., Santangelo, E., Gulletta, E., Fuiano, G., Costanzo, F.S., Renzulli, A., 2009. Pulsatile perfusion with intra-aortic balloon pumping ameliorates whole body response to cardiopulmonary bypass in the elderly. *Critical Care Medicine*, 37(3), 902-911.

Onorati, F., Santarpino, G., Rubino, A., Cristodoro, L., Scalas, C., Renzulli, A. 2009. Intraoperative bypass graft flow in intra-aortic balloon pump-supported patients: differences in arterial and venous sequential conduits. *Journal of Thoracic Cardiovascular Surgery*, 138(1), 54-61.

Onorati, F., Santarpino, G., Rubino, A.S., Caroleo, S., Dardano, A., Scalas, C., Gulletta, E., Santangelo, E., Renzulli, A., 2009. Body perfusion during adult cardiopulmonary bypass is improved by pulsatile flow with intra-aortic balloon pump. *International Journal of Artificial Organs*, 32(1), 50-61.

Papademetriou M. D. 2011. *Multichannel Near Infrared Spectroscopy to monitor cerebral oxygenation in infants and children supported in extracorporeal membrane oxygenation (ECMO).* Thesis (Ph.D). University College London.

Ma P., Zhang Z., Song T., Yang Y., MSa, Meng G., Zhao J., Wang C, Gu K., Peng J., Jiang B., Qi Y., Yan R., Ma X., 2014. Combining ECMO with IABP for the Treatment of Critically Ill Adult Heart Failure Patients. *Heart, Lung and Circulation*, 23, 363–368.

Quarteroni A., Tuveri M., Veneziani A., 2000. Computational Vascular Fluid Dynamics: problems, models and methods. *Computing and Visualization in Science*, 2, 163-197.

Vignon-Clementel I. E., Figueroa C. A., Jansen K. E., Taylor C. A., 2006. Outflow boundary conditions for three dimensional finite element modeling of blood flow and pressure in arteries. *Computer Methods in Applied Mechanics and Engineering*, 195, 3776–3796.

Vignon-Clementel, I., 2006. *A couple multidomain method for computational modeling of blood flow*, Thesis (PhD). Stanford University.